Fluid Structure Interaction of Oscillating Elastic Plates

By:

Rushikesh Deotale

Department of Mechanical Engineering

BITS Pilani

Project carried out under the SURGE Program at IIT Kanpur

Under the guidance of

Dr Murali Damodaran and Dr Pradeep Moise

Department of Aerospace Engineering
IIT Kanpur

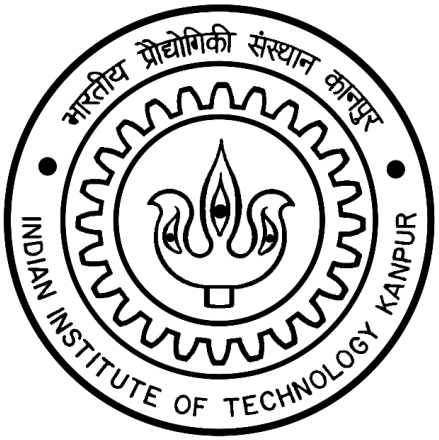

Abstract

This research focuses on investigating the Fluid-Structure Interaction (FSI) of oscillating elastic plates to understand the complex dynamics and aeroelastic instabilities using computational techniques based on the finite volume technique for both solid mechanics and fluid dynamics. The study aims to achieve three objectives. Firstly, it verifies the reliability and limitations of the *Solids4foam* solver, which uses a finite volume method in *OpenFOAM* for solving solid mechanics equations and overset meshes for FSI studies. Secondly, it aims to make predictions for plate deformation, von-Neumann stress and strain fields, unsteady aerodynamic forces, unsteady ambient flowfields and vortex shedding. The computed results are then visualised to identify interesting characteristics and calculate aeroelastic parameters.Insights from this research can support the understanding of flexible aircraft structures, such as large aspect ratio elastic wings for aerial vehicles, and also advances partitioned computational aeroelasticity. The study presents an efficient method for examining the effects of fluid flow on oscillating plates by utilising overset and dynamic mesh. It is easier to comprehend aeroelastic phenomena and create more resilient structures with accurate calculation of aerodynamic plate deformation and structural stress fields. The effort will add to the body of knowledge in the discipline and have implications for handling more challenging issues and advancing computational aeroelasticity.

Keywords- Solids4Foam, Fluid-Structure Interaction, Computational Aeroelasticity.

ACKNOWLEDGMENTS

No great work can be done well without the support and guidance of a great mentor. I could not have written this report without the assistance of my instructors, Dr Murali Damodaran and Dr Pradeep Moise, who were always available and served as a guiding light for us. The completion of this project report owes much to the concepts and teachings they provided, as well as their diligent efforts in addressing our doubts about the simulations involved. The report would not have progressed to its completion state without their support.

TABLE OF CONTENTS

1. Introduction

Fluid-Structure Interaction (FSI) is a phenomenon that occurs when a fluid interacts with a solid structure, resulting in complex dynamics and aeroelastic instabilities. The understanding and analysis of FSI phenomena are crucial in various engineering applications, such as aerospace, civil engineering, and biomechanics. Computational techniques have emerged as powerful tools for investigating and predicting the behavior of FSI systems, enabling engineers and researchers to gain valuable insights and optimize the design and performance of such systems.

This research paper focuses on the investigation of the Fluid-Structure Interaction of oscillating elastic plates using computational techniques based on the finite volume method. The study aims to understand the complex dynamics and aeroelastic instabilities that arise in such systems and provide insights into their behavior under different loading conditions. The Solids4foam solver, which utilizes the finite volume method in OpenFOAM for solving solid mechanics equations and overset meshes for FSI studies, is employed as the primary computational tool in this research.

The objectives of this study can be summarized into three main aspects. Firstly, the reliability and limitations of the Solids4foam solver are verified to ensure its suitability for simulating the FSI behavior of oscillating elastic plates. This involves assessing the solver's accuracy in capturing the complex interactions between the fluid and the structure and evaluating its performance in various scenarios.

Secondly, the study aims to make predictions for different parameters associated with plate deformation, stress and strain fields, unsteady aerodynamic forces, unsteady ambient flowfields, and vortex shedding. These predictions provide valuable insights into the behavior and characteristics of FSI systems, allowing for a better understanding of the underlying physical processes.

Lastly, the computed results are visualized to identify interesting characteristics and calculate aeroelastic parameters. Visualization techniques enable researchers to gain a comprehensive understanding of the FSI behavior by observing the flow patterns, stress distributions, and other relevant parameters. Additionally, the calculation of aeroelastic parameters provides quantitative measures for evaluating the performance and stability of oscillating elastic plates under fluid-structure interactions.

To achieve these objectives, the Solids4foam solver is utilized to simulate the FSI behavior of oscillating elastic plates. The solver employs the finite volume method, a widely used numerical technique for solving partial differential equations, to discretize and solve the governing equations of solid mechanics and fluid dynamics. The use of morphing meshes facilitates the accurate representation of the moving boundaries and the interaction between the fluid and the structure.

The investigation focuses on analyzing the temporal variation of tip displacement, stress distribution, and fluid flow characteristics of the oscillating elastic plates. These parameters provide valuable insights into the structural behavior, energy dissipation, and aerodynamic effects of the plates during the oscillation process. The analysis of vortex shedding, pressure distribution, and stress variations allows for a deeper understanding of the complex dynamics and aeroelastic instabilities inherent in FSI systems.

The findings of this research study contribute to the existing body of knowledge in the field of FSI analysis. The insights gained from the computational simulations and visualizations offer valuable information for engineers and researchers to optimize the design, improve the performance, and mitigate potential instabilities in various engineering applications. Moreover, the validation and verification of the Solids4foam solver provide a reliable computational tool for future FSI studies.

2. Mathematical Model for Fluid-Structure Interaction

The research focuses on the fluid-structure interaction (FSI) of an oscillating elastic aluminum plate submerged in an ambient quiescent fluid. The objective is to test the *Solids4Foam* solver, an extension of the *OpenFOAM* software,to simulate the behavior of the plate as it undergoes oscillations after being initially displaced by a uniform load.

2.1 Problem Definition

This research work aims to provide a detailed investigation of the fluid-structure interaction of an oscillating elastic aluminum plate using the *Solids4Foam* solver. The subsequent sections will delve into the mathematical models, numerical methods, and results obtained from the simulation, shedding light on the behavior and performance of the developed solver in capturing the intricate phenomena associated with FSI.

To initiate the simulation, an appropriate computational domain was defined. The fluid domain (*Fig 1 (a)*) is characterised by its width (*w*), length (*l*), and height (*h*), while the cuboid plate (*Fig 1 (b)*) exhibits high aspect ratio dimensions of length (L), thickness (H), and width (W). The plate is fixed to face ABCD of the fluid domain from its base, located at the center of face ABCD. Simultaneously, the top surface of the plate is positioned M*1 distance away from face EHGF of the fluid domain, creating a non-parallel configuration. Table 1 provides the dimensions of the fluid and solid domains, along with the mechanical properties of aluminium.

For fluid Domain, value of Length (*l*) is 3m, width (*w*) is 2m and height (*h*) is 2m. For solid domain (rectangular thin plate), value of Length (L) is 1m, Width (W) is 0.4m and Height (H) is 0.05m. Rectangular plate is made up of Aluminium with modulus of elasticity of 68 GPa, Density of 2.7 g/cc and Poissons ratio of 0.33. Uniform structured rectangular mesh of 0.001m was used to mesh both Fluid as well as Solid Domain.

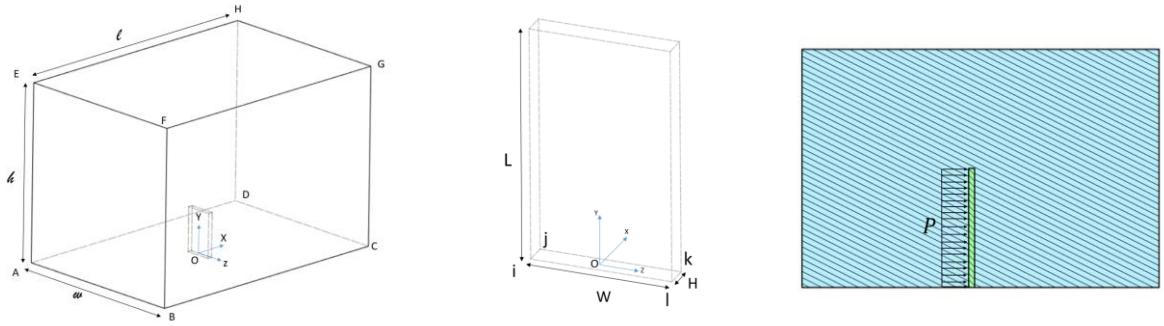

(a) (b) (c)

Fig 1. *(a) Fluid Domain,(b) Solid Domain (Rectangular thin plate), (c) Uniform load over the plate*

The initial displacement of the plate is achieved by applying a uniform load *P* (Fig1 (c)) . After a defined time duration t, the load is removed, allowing the plate to oscillate freely in the fluid. The visualization of deformation, stress, velocity, vortex patterns, and pressure will provide a comprehensive

2.2. Mathematical Model and Boundary Conditions

2.2.1. Governing Equations

In the current study, an FV discretization and a partitioned technique are used to examine the interaction between an incompressible Newtonian fluid and a hyperelastic solid. Separate mathematical models describing the mechanical behaviour of the fluid and the solid are solved, and coupling is accomplished at the contact by enforcing appropriate boundary conditions. The deformation of the fluid-solid interface is taken into account when considering fluid flow on a spatial domain whose shape is changing over time. Isothermal flow of a Newtonian fluid that is incompressible, inside of any volume V that is bordered by a closed moving surface S. the solid's assumed to be elastic and compressible deformation. Kinematic and dynamic requirements that must be met at the fluid-solid interface connect the fluid and solid models. In further sub-sections Mathematical Equations for Fluid domain, Solid domain and Coupling conditions would be discussed in detail.

2.2.1.1 Fluid Equations

The governing equations are the Navier–Stokes equations in the Cartesian coordinates. The governing equations are non-dimensionalised by a fluid density , a characteristic velocity U and a characteristic length L

$$\nabla \cdot u = 0 \tag{1}$$

$$\frac{\partial u}{\partial t} + (u \cdot \nabla)u = -\frac{1}{\rho}\nabla P + \nu \nabla^2 u \tag{2}$$

2.2.1.2 Plate Equations

The wing's flapping motion causes a significant traverse deflection in the spanwise direction. The Kirchoff thin plate theory can be used to simulate this deflection when the wing is narrow.

$$D\nabla^2\nabla^2 w(y,z,t) = p(y,z,t) - \rho h \frac{d^2 w}{\partial t^2}(y,z,t). \tag{3}$$

for natural or free vibrations, $p(y,z,t)$ is set equal to zero in (2), and thus Eq (2) becomes

$$D\nabla^2\nabla^2 w(y,z,t) + \rho h \frac{d^2 w}{\partial t^2}(y,z,t) = 0 \tag{4}$$

$$D = \frac{Eh^3}{12(1-v^2)}$$

where,

$w(x,y,t), \rho, h$ *are,* respectively, deformation, density and thickness of plate of the plate .

Boundary conditions for a clamped end at y = 0 and a free end at y = L are given as follows:

$$w(0,z,t) = 0 \text{ and } \frac{\partial w}{\partial n} = 0$$

where n is in the direction normal to the edge of the plate under consideration.

The deformation of the solid is assumed to be elastic and compressible. From the definitions of the strain components we find then that

$$\varepsilon_{zz} = -x\frac{\partial^2 w}{\partial z^2}, \quad (5a)$$

$$\varepsilon_{yy} = -x\frac{\partial^2 w}{\partial y^2}, \quad (5b)$$

$$\gamma_{zy} = -2x\frac{\partial^2 w}{\partial z\,\partial y} \quad (5c)$$

From Hooke's law

$$\varepsilon_{zz} = \frac{1}{E}(\sigma_{zz} - v\sigma_{yy}), \quad (6a)$$

$$\varepsilon_{yy} = \frac{1}{E}(\sigma_{yy} - v\sigma_{zz}), \quad (6b)$$

$$\gamma_{zy} = \frac{2(1+v)}{E}\sigma_{zy} \quad (6c)$$

we get the stress components

$$\sigma_{zz} = \frac{E}{1-v^2}(\varepsilon_{zz} + v\varepsilon_{zy}) = -\frac{Ez}{1-v^2}\left(\frac{\partial^2 w}{\partial z^2} + v\frac{\partial^2 w}{\partial y^2}\right), \quad (7a)$$

$$\sigma_{yy} = \frac{E}{1-v^2}(\varepsilon_{yy} + v\varepsilon_{zz}) = -\frac{Ez}{1-v^2}\left(\frac{\partial^2 w}{\partial y^2} + v\frac{\partial^2 w}{\partial z^2}\right), \quad (7b)$$

$$\sigma_{zy} = \frac{E}{2(1+v)}\varepsilon_{zy} = -\frac{Ez}{1+v}\frac{\partial^2 w}{\partial z \partial y}. \quad (7c)$$

The stress components change linearly with plate thickness, just like the strain component variations do. It follows from these equations that the most important stress and strain components can be calculated if we know the plate's deflection.

The Kirchhoff-Love theory predicts a zero distribution of shear stresses along the x direction. Thus, it can only be applied in problems where the variation of such stresses is expected to be small and their mean value does not deviate from 0. Such can be considered the case of thin plates as discussed by Tuković et al. [1].

The effects of fluid loading on plate

The fluid causes the plate to experience more inertia loading, which lowers the plate resonant frequencies. The fluid is exposed to acoustic energy from the vibrating plate, and this loss of vibrational energy adds a resistive term to the plate's impedances.

According to Wu et al. [2], the three-dimensional Helmholtz wave equation governs the acoustic velocity field caused by plate motion.

$$\nabla^2\Phi(x,y,z,t) = \frac{1}{c^2}\frac{\partial^2\Phi(x,y,z,t)}{\partial t^2} \tag{8}$$

where ∇^2 is the three-dimensional Laplacian operator, c is the velocity of sound within fluid and $\Phi(x,y,z,t)$ is the velocity potential of the fluid. Boundary conditions(continuity of normal velocity) at the interface between the fluid and the baffled plate $(z=0)$ can be expressed as: $\partial\Phi/\partial z|_{z=0} = \partial w/\partial t$ on the plate

For a steady-state response in harmonic motion, the acoustic velocity potential becomes $\Phi(x,y,z,t) = \phi(x,y,z)e^{-i\omega t}$. where $\phi(x,y,z)$ is the spatial velocity potential function.

The fluid-induced inertial effect on the plate can be represented by added mass factor (β_{mn}) or NAVMI factor (Γ_{mn}). which is simply the function of plate natural modes. They are defined as follows

$$\beta_{mn} = \left(w_{v,mn}/w_{f,mn}\right)^2 - 1 = \Gamma_{mn}\frac{\rho_f e L_b}{\rho_p h} \tag{9}$$

where $w_{v,mn}$ and $w_{f,mn}$ are the natural frequencies of plate in vacuo and in fluid respectively, ρ_f is the density of fluid, ε is the plate aspect ration L_b/L_a. From the view of energy, the added mass effect can be evaluated as proportional to the kinetic energies of the fluid (T_f), which is defined as

$$T_f = -\frac{1}{2}\rho_f\int_{-\infty}^{\infty}\int_{-\infty}^{\infty}\left.\frac{\partial\phi(x,y,z)}{\partial z}\right|_{z=0}\phi(x,y,0)dxdy \tag{10}$$

2.2.2. Initial Condition

Initially, the cantilever plate is in a resting horizontal position within a ambient quiescent fluid. A uniform load of $P$is gradually applied in the positive X direction onto the front face of the plate (Fig 1 (c)). The load $P$is incrementally increased from 0 N to 60kN over a period of 0.2 seconds to prevent any potential fluid shock. From 0.2 seconds to 4 seconds, a uniform load of 60kN is continuously applied. The force $P$is counteracted by the stress generated within the plate, causing it to reach its final displaced position at 2.5 seconds. At 4 seconds, the uniform loading of P is removed.

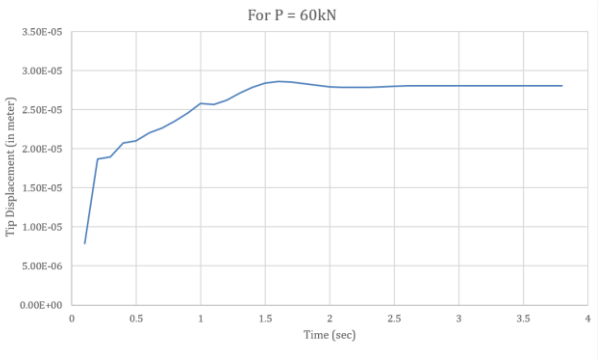

Fig 2 . *Initial Tip displacement vs Time for uniform loading of P= 60kN*

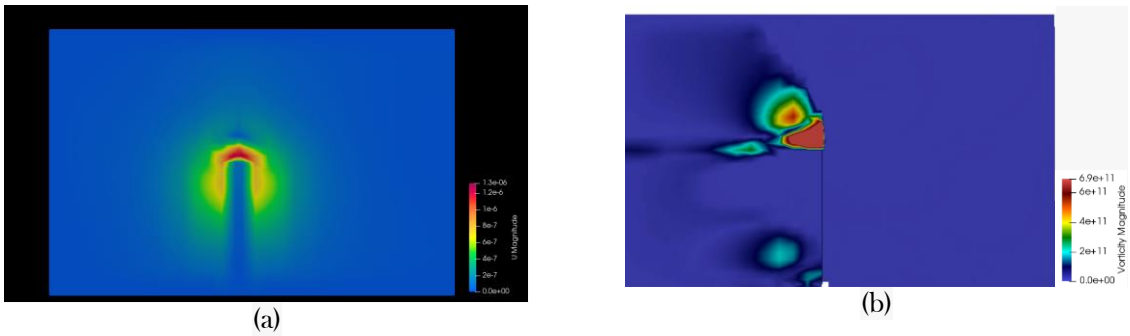

(a) (b)

Fig 3 . *(a) Velocity contour and (b) Vorticity contour at initial position of plate (t = 3.8 sec)*

In order to attain the initial condition, a uniform load was applied for a duration of 3.9 seconds. Fig 3 (a) illustrates the velocity contour resulting from the disturbance caused by the displacement of the plate due to the uniform load. Likewise, Fig 3 (b) portrays the vortex generated as a result of the plate displacement caused by the uniform load to reach initial position.

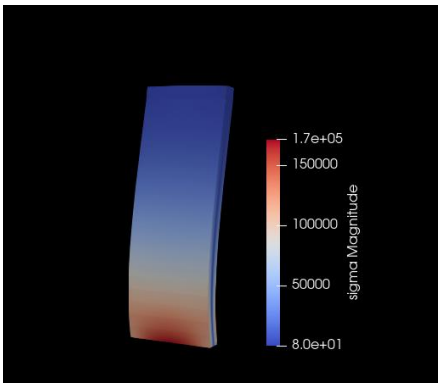

Fig 4 .*Stress contour at initial position of plate (t = 3.8 sec)*

Fig 4 represents the stress distribution at the initial position of the system. At the clamped end, a maximum stress of $1.6*10^5$ units was observed. This stress arises as a result of the counteraction of the uniform loading of P = 60kN by the elastic properties of the plate. Consequently, the plate remains at rest in its initial position.

2.2.2. Boundary Conditions

2.2.2.1 Fluid Domain

The fluid problem is endowed with a Dirichlet boundary condition for velocity at the fluid-structure interface, enforcing the kinematic coupling condition that is value of u, v, w would be adjusted according to the new moving wall velocity.

Pressure on surface ABFE, EFGH, HGCD, EHDA, FGBC and ABCD as shown in fig1 = $\boldsymbol{P}_{\infty}$

Pressure boundary condition at interface from fluid domain: $\nabla P \cdot n = 0$

The equation $\nabla P \cdot n = 0$ represents the zero-gradient condition for pressure, where ∇P is the pressure gradient and n is the outward unit normal vector to the fluid-structure interface.

In the fluid domain, the relative velocity components $u_f - u_s$, $v_f - v_s$, and $w_f - w_s$ are set to zero, where u_f, v_f *and* w_f represent the fluid velocities in the x, y, and z directions, respectively and u_s, v_s *and* w_s represent the plate velocities in the x, y, and z directions, respectively.

2.2.2.2 Solid Domain

The dynamic coupling condition is enforced by adding a Neumann boundary condition (traction) at the interface to the structural domain. Force (traction) is typically calculated at the fluid side of the interface and applied as a boundary condition at the solid side of the interface in the partitioned computational technique. According to Girfoglio et al. [3], the traction is estimated using the fluid stress tensor, which includes isotropic and viscous components. According to Newton's rule of viscosity, the viscous (deviatoric) component is:

$$f = \mu[\nabla \mathbf{v} + \nabla \mathbf{v}^{\mathrm{T}}] \tag{11}$$

where $\mu = \rho\nu$ is the fluid dynamic viscosity. Hence, the stress tensor for an incompressible Newtonian fluid reads as follows:

$$\sigma_{F,i} = -p\mathbf{I} + \tau = -p\mathbf{I} + \mu[\nabla \mathbf{v} + \nabla \mathbf{v}^{\mathrm{T}}]. \tag{12}$$

and the traction at the interface reads:

$$\mathbf{t}_{F,i} = \mathbf{n}_i \cdot \sigma_{F,i} = -p\mathbf{n}_i + \mu\mathbf{n}_i \cdot \nabla \mathbf{v}_t - 2\mu(\nabla_s \cdot \mathbf{v})\mathbf{n}_i + \mu\nabla_s v_n, \tag{13}$$

where $\mathbf{v}_t = (\mathbf{I} - \mathbf{nn}) \cdot \mathbf{v}$ is the tangential velocity component, $\nabla_s = \nabla - \mathbf{nn} \cdot \nabla$ is the surface tangential gradient operator and $v_n = \mathbf{n} \cdot \mathbf{v}$ is the normal velocity component. On the right hand side of the equation, the third and fourth terms can typically be ignored; if not, these terms can be calculated directly at the solid side of the contact assuming that the kinematic condition is true.

2.2.3. Coupling conditions

The fluid dynamics and structural dynamics governing equations, which were developed in the Eulerian and Lagrangian frameworks, respectively, must be modified for FSI. Because the fluid mesh deforms over time as a result of the interactions between forces passed by the fluid to the structure and displacement sent back

to the fluid by the solid, as the large grid distortions in the solid (caused by the large deformations from the fluid) occur, this can result in the destruction of the structural mesh.
As a result of the fluid mesh deformation in the ALE technique, an observer is neither immobile in space nor moves with a material point. Instead, the observer is free to move in any direction at whim. In order to put this idea into practise, the Leibnitz rule is utilised to alter the fluid integral conservation equations, which are the conservation equations for mass and momentum. Their ALE formulations therefore include a fresh set of conservation equations developed by Priambudi et al. [4]

$$\frac{d}{dt}\int_{V(t)} \rho_f dV + \int_{S(t)} \rho_f (u - u^g)\cdot ndS = 0 \qquad (14a)$$

$$\frac{d}{dt}\int_{V(t)} \rho_f dV + \int_{S(t)} \rho_f (u - u^g)\cdot ndS = -\int_{S(t)} pnds + \int_{V(t)} \mu_f(\nabla u + (\nabla u)^T)dV + \int_{V(t)} \rho_f b dV \qquad (14b)$$

Equations (10a) and (10b) introduce the velocity of the time-dependent surface of the control volume (CV) or the velocity of the moving grid u^g in order to translate the fluid velocity into a moving reference system. Equations (10a) and (10b) are consequently transformed into the Navier-Stokes equations in the Eulerian description when the grid velocity is u^g=0 and the Lagrangian formulation when u^g=u. For the purpose of computing convective fluxes at the CV cell faces, the equations now include a relative velocity, u-u^g. When the faces of CV move in the FSI simulation, extra mass fluxes are injected, indicating that the mass balance is not always guaranteed.
The space conservation law (SCL), which is as follows, must be used in the revised conservation equations to avoid the mass imbalance.

$$\frac{d}{dt}\int_{V(t)} dV + \int_{S(t)} u^g \cdot ndS \qquad (15)$$

Equation (11) guarantees that the rate of change of the volume itself is equal to the total of fluxes through the faces of CV as a result of the grid deformation.
The fluid and solid governing equations are coupled by the kinematic and dynamic coupling conditions at the fluid-structure interface I(t). The kinematic condition ensures constant displacement and velocity across the interface:

$$u_f|_{I(t)} = u_s|_{I(t)}, \qquad d_f|_{I(t)} = d_s|_{I(t)} \qquad (16)$$

The dynamic condition employs the equilibrium of the forces at the interface:

$$n_I \cdot \sigma_f = n_I \cdot \sigma_s \qquad (17)$$

where n_I is the unit normal vector at the interface.

In the FSI simulation, the transfer of the forces from the fluid part and of the displacement from the solid part takes place on the interface.

2.3 . *Solids4foam* Workflow

The solids4foam project aims is to develop an OpenFOAM toolbox for solid mechanics and fluid-solid interactions. Similar to the traditional OpenFOAM solvers, solids4Foam requires the same case preparation. OpenFOAM and solids4Foam use a similar directory structure. Different solvers in OpenFOAM have hard-coded versions of many mathematical models. For instance, icoFoam cannot be used to simulate a compressible flow because it uses the reduced Navier-Stokes model for incompressible flows as its implemented model. Similar to this, as the Navier-Stokes equations included in this solver are streamlined for steady flows, simpleFoam cannot be utilised to model an unsteady turbulent flow. When a solver is called through the terminal in OpenFOAM, the solver's particular implementation is run. However, there is just one solids4Foam solver in the programme. Each model for a solid or fluid is implemented within a particular class. This modular approach of the solver was described in detail by Shayegh [4], and when solids4Foam is executed for a specific problem, it reads the model(s) specified by the user and then calls for the related class(es) (as shown in fig. 5). As a result, the models are run-time selectable rather than being hard-coded within the solver.

In the context of this research, the focus is on simulating the fluid-structure interaction of an oscillating elastic aluminum plate.

The investigation involves the initial displacement of the plate using a uniform load, followed by the removal of the load to allow the plate to oscillate in an ambient quiescent fluid. This scenario represents a fundamental problem in FSI and serves as a basis for studying the behavior and performance of the developed solver.

A partitioned technique is used to analyse the interaction between the elastic solid and the incompressible Newtonian fluid. Separate mathematical models for the solid's and fluid's mechanical behaviour are solved, and the coupling is accomplished by imposing the right boundary conditions at the fluid-solid interface. The motion of the fluid-solid interface causes a spatial domain in which the fluid flow takes place to deform over time. The linear momentum conservation law in the total Lagrangian form, as developed by Wu et al. [1], is used to describe the deformation of the solid material, which is assumed to be elastic and compressible.

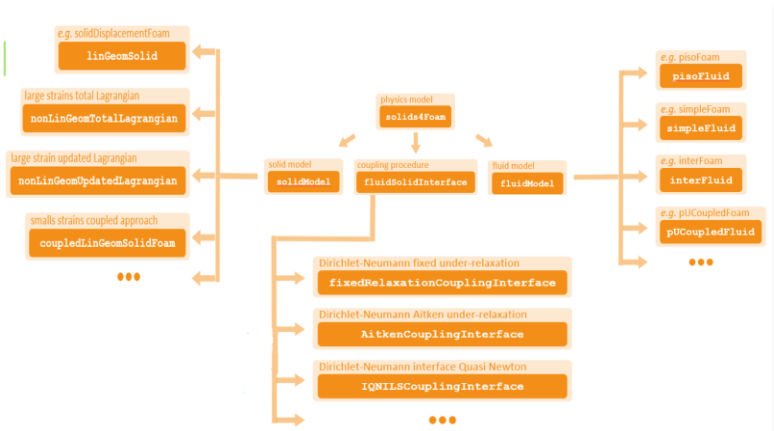

Fig 5. Flowchart of modular approach of solids4foam

Tuković et al. [6] mentioned that in the partitioned computational approach, the traction (force) is calculated on the fluid side of the interface and applied as a boundary condition on the solid side. The traction is calculated using the fluid stress tensor, which has both isotropic and viscous components. Iterative processes are used to achieve the connection between the fluid and solid domains, ensuring accurate and reliable information flow.

3. Results and Discussion

This section presents the results obtained from the computational simulations conducted to investigate the Fluid-Structure Interaction (FSI) of oscillating elastic plates. The results are organised into three subsections, focusing on (a) Temporal Variation of Tip Displacement and Stress of the plate, (b) the computed vortex lines around the plate, and (c) the characteristics of the Fluid-Structure Interaction.

3.1. Temporal variation of Tip Displacement and Stress in The Plate.

The first set of results focuses on the temporal variation of the tip displacement and stress of the plate. Fig 6 (a) and Fig 6 (b) illustrate the tip displacement of the plate under two different uniform loading conditions: P= 60 kN and P= 60,000 kN. Fig 7 presents the temporal variation of average stress at the clamped end of the plate during the oscillations.

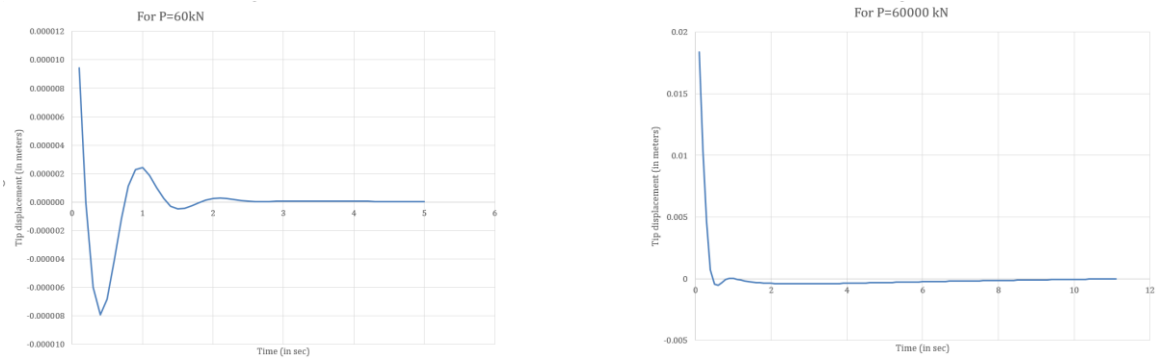

(a) (b)

Fig 6. *Tip displacement vs Time for uniform loading of (a) P = 60 kN (b) P = 60000 kN*

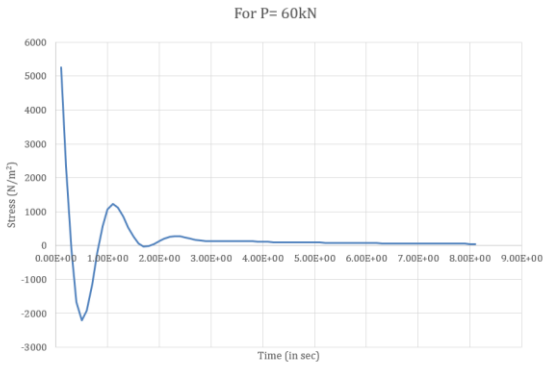

Fig 7 *Average Stress over the area at the clamped end of the rectangular plate vs Time*

It can be observed from Fig 6 that the amplitude of oscillation decreases over time due to the damping effect of the fluid. Furthermore, a notable observation is that the oscillations are not as prominent for the case of P= 60,000 kN compared to P= 60 kN. Therefore, further analysis will focus only on the results obtained for the P= 60 kN case.

The stress values are plotted against time (Fig 7), allowing for the analysis of stress changes as the plate undergoes oscillatory motion.

3.2. Computed Vortex lines

The second set of results focuses on the computed vortex lines around the plate. Fig 8 (a) depicts the vortex lines at t = 4.2 sec, which is 0.3 sec after the plate was released from its initial position. Fig 8 (b) shows the vortex lines when the plate reaches its amplitude position (t = 5 sec)

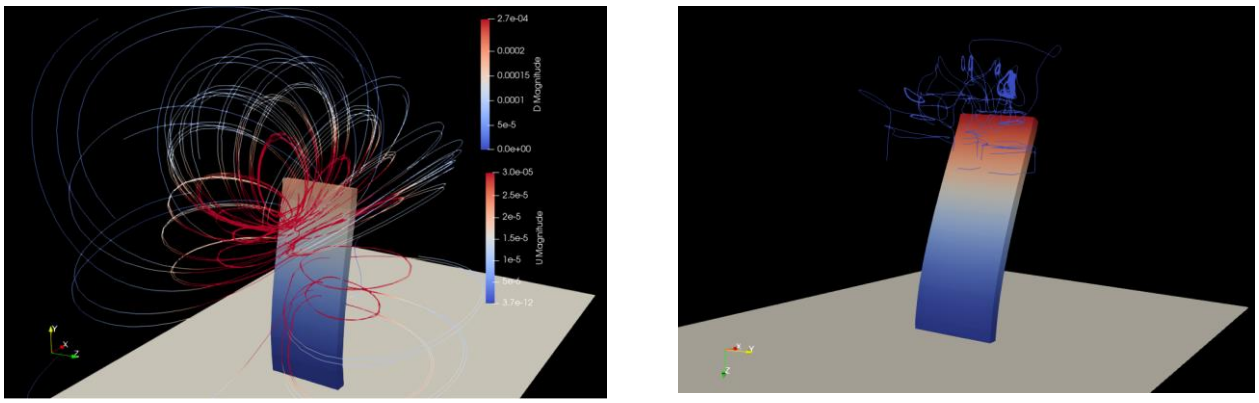

(a) (b)

Fig 8. *Computed vortex-lines at instant (a) t= 4.2 sec (b) t = 5 sec*

The vortex lines are prominent as the plate travels from its initial position, displacing the fluid in its path (Fig 8 (a)). At the amplitude position (Fig 8 (b)), the velocity of the plate reduces to zero, resulting in less prominent vortex lines compared to Fig 8 (a). These visualizations of the vortex lines provide insights into the fluid flow patterns and the interaction between the plate and the surrounding fluid.

3.3 Characteristics of Fluid-Structure Interaction

The third set of results focuses on the characteristics of the Fluid-Structure Interaction, including vorticity, pressure exerted by the fluid on the plate, and stress in the plate at specific time instances. These results are presented for t = 4.1 sec, t = 4.6 sec, and t = 9 sec. The plate is released from its initial position at t = 3.9 sec and starts moving towards its equilibrium position. At t = 4 sec, the plate is in transit towards the equilibrium position, and at t = 4.5 sec, it reaches its amplitude position. At t = 9 sec, the amplitude of the plate has significantly reduced due to damping effects.

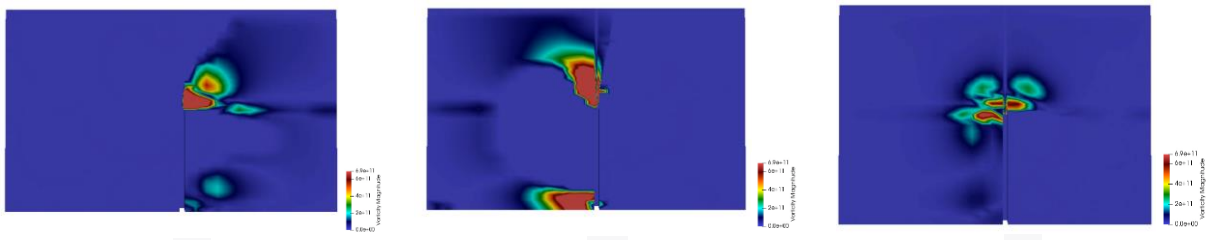

(a) (b) (c)

Fig 9. *Time evolution of the vorticity contours (a) t = 4 sec (b) t = 4.6 sec (c) t = 9 sec*

Fig 9 (a) illustrates the vorticity behind the plate as it moves towards its equilibrium position, 0.2 sec after release. The vorticity contours provide valuable information about the flow patterns generated by the plate's motion. In Fig 9 (b), motion of plate is from its extreme position to its equilibrium position (direction of motion is opposite to that of the plate in Fig 9 (a)). Lastly, Fig 9 (c) presents the vorticity distribution at t = 9 sec, when the oscillations have nearly damped down. The formation of less intense vortices compared to the earlier cases suggests that the oscillations have been significantly reduced.

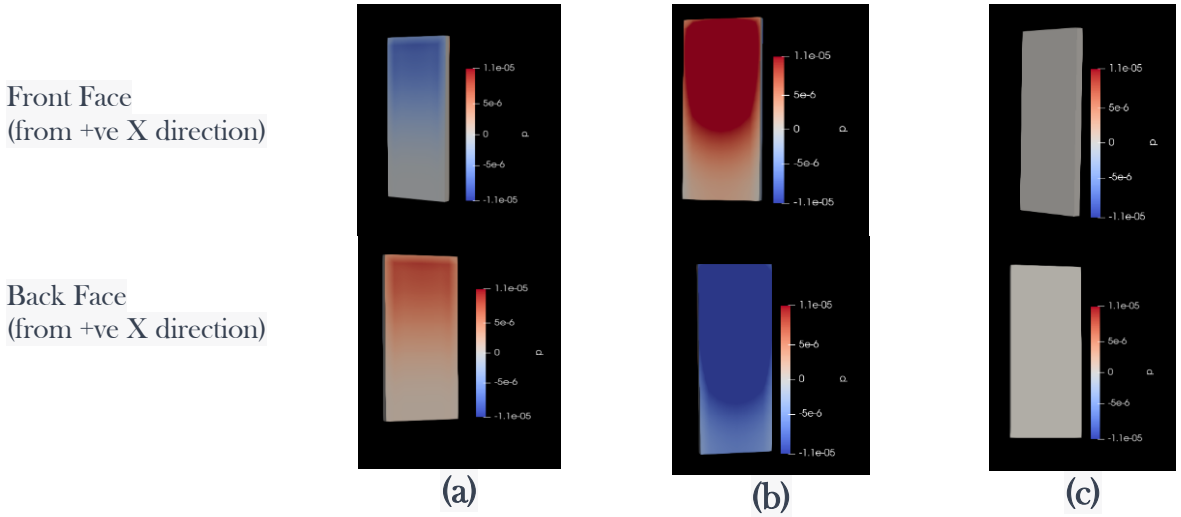

Fig 10. *Pressure exerted by Fluid on plate (a) t = 4 sec (b) t = 4.6 sec (c) t = 9 sec*

Furthermore, the pressure exerted by the fluid on the plate is investigated. Fig 10 (a) depicts the pressure distribution at t = 4.5 sec, when the plate is traveling in the opposite direction from the other extreme end. It can be observed that the pressure is higher on the front side (in compression) compared to the back side (in tension). In Fig 10 (b) pressure distribution is the opposite of what was observed in Fig 10 (a) as at t = 4.6 sec, plate is traveling from extreme position to equilibrium position but in opposite direction of motion of plate in Fig 10 (a) . Lastly, Fig 10 (c) pressure distribution at t = 9 sec, when the oscillations have nearly damped down. Consequently, the pressure exerted by the fluid on the solid structure in this case is negligible compared to the earlier cases.

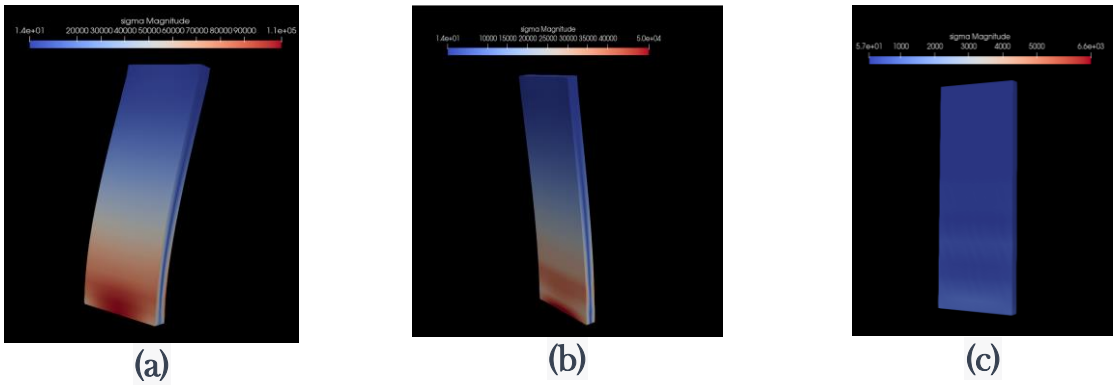

Fig 11. *Stress contours of plate (a) t= 4 sec (b) t = 4.6 sec (c) t= 9 sec*

Additionally, the stress distribution in the plate is analyzed at the aforementioned time instances (Fig 11). It is observed that the stress is higher at the clamped end of the plate and gradually reduces as we move

towards the free end. This stress distribution pattern provides valuable insights into the structural behavior of the oscillating plate under fluid-structure interaction.

Overall, the results obtained from the computational simulations provide valuable information regarding the temporal variation of tip displacement and stress of the plate, the computed vortex lines around the plate, and the characteristics of the fluid-structure interaction. These findings contribute to a deeper understanding of the complex dynamics and aeroelastic instabilities associated with oscillating elastic plates and their interaction with the surrounding fluid.

3.4 Convergence Analysis

Convergence analysis was performed to ensure the reliability of the Solids4foam solver in accurately capturing the Fluid-Structure Interaction (FSI) behavior of oscillating elastic plates. The analysis focused on monitoring the convergence of key variables, including Ux, Uy, Uz, and p, which represent the velocity components and pressure, respectively.

Convergence was evaluated through the examination of residue plots, which provide insights into the reduction of errors in the numerical solution as the number of iterations progresses. Each time step in the simulation consisted of 20 iterations. Total there are 150 time steps which make up total of 3000 iterations. The tolerance level, set at 10^{-6}, served as the criterion for convergence. The residue values, representing the difference between consecutive iterations, were compared to the tolerance level to determine the convergence status.

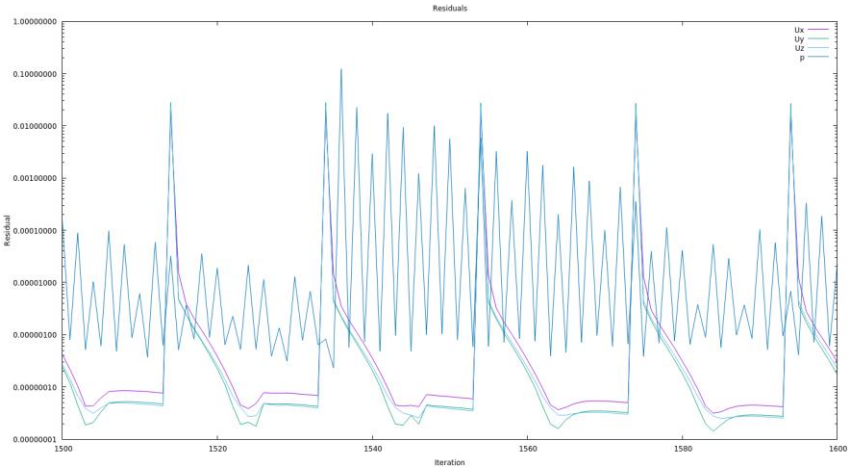

Fig 12*. Residual values of Ux, Uy and p from 1500 to 1600 iterations*

The residue plots for Ux, Uy, Uz, and p were monitored at each time step. The progression of residue values over the iterations was observed to assess the stability and accuracy of the simulations. As the iterations advanced, the residue values progressively decreased, indicating the convergence of the numerical solution. In Fig 12, iterations from 1500 to 1600 were analysed, similar pattern was observed from iteration 0 to iteration 3000.

5. Conclusion and Further Work

Based on the observations made, several conclusions can be drawn. Firstly, it was observed that the amplitude of plate oscillations is more prominent for smaller initial loading compared to larger initial loads. This can be attributed to the dissipation of energy to the surrounding fluid, which is more significant for larger displacements. As a result, the vibrations become less prominent as the energy dissipation increases with larger initial loads. Furthermore, from the analysis conducted in section 2.1, it can be concluded that the stress in the plate varies proportionally to the displacement of the plate. As the displacement increases, so does the stress experienced by the plate. This finding highlights the direct relationship between plate displacement and stress distribution. The vorticity contours obtained from section 2.3 revealed that as the plate travels from its amplitude position to its equilibrium position, it generates a wake behind it, resulting in vortex shedding. It was observed that the intensity of these vortices decreases with time, corresponding to the decrease in plate amplitude. Moreover, the pressure exerted by the fluid on the plate and the von-Neumann stress distribution were analysed. It was observed that the pressure exerted by fluid on plate is higher on the compressed side of the plate compared to the tension side. Additionally, both the pressure and stress experienced by the plate decrease over time as the plate's amplitude decreases due to damping effects.

Further work

Based on the findings and insights obtained from this research, there are several avenues for future work to expand upon and enhance the understanding of FSI phenomena in oscillating elastic plates.

One direction for further research would be to analyze the twisting motion of the plate. By applying a moment to the tip of the plate and releasing it from its initial twisted position, the characteristics of the Fluid-Structure Interaction during twisting motion could be investigated. Similar analysis techniques, such as examining vorticity and pressure contours in the fluid domain, as well as studying the temporal variation of stress, displacement, and pressure exerted by the fluid on different parts of the plate, could be employed. This extension would provide insights into the behavior and stability of oscillating plates under twisting motion, complementing the existing knowledge on bending motion.

Furthermore, future studies could consider the combined effect of twisting moments and bending forces on the plate. By applying both twisting moment and bending force to bring the plate into its initial position within the fluid and subsequently releasing it from rest, the Fluid-Structure Interaction characteristics could be observed and analyzed. This comprehensive investigation would provide a deeper understanding of the complex dynamics and aeroelastic instabilities arising from the combined loading conditions.

6. Appendix

Installation and Setup of *solids4Foam* Solver in *OpenFOAM* v1912 and Foam-Extend 4.0 on PARAM Sangnak Supercomputer

In this appendix, we provide detailed instructions on how to install and set up the solids4Foam solver in *OpenFOAM* v1912 and Foam-Extend 4.0 on the PARAM Sangnak supercomputer.

1. Installing and Setting up *OpenFOAM* v1912 on PARAM Sangnak Supercomputer:

1.1. Log in to your PARAM account and create a folder called *OpenFOAM*.

1.2. Download the *OpenFOAM* v1912 source files from the following URLs:

- *OpenFOAM*: https://sourceforge.net/projects/openfoam/files/v1912/OpenFOAM-v1912.tgz
- Third-party packages: https://sourceforge.net/projects/openfoam/files/v1912/ThirdParty-v1912.tgz

1.3. Extract the downloaded files using the following commands:

```
tar -xzf OpenFOAM-v1912.tgz
tar -xzf ThirdParty-v1912.tgz
```

1.4. Open the .bashrc file in your home directory using the command **nano .bashrc**. 1.5. Modify the .bashrc file, after modyfing bashrc, it should look like this:

```
# .bashrc
# Source global definitions
if [ -f /etc/bashrc ]; then
    . /etc/bashrc
fi

# Uncomment the following line if you don't like systemctl's auto-paging
feature:
# export SYSTEMD_PAGER=

# User-specific aliases and functions
module load compiler/openmpi/gcc/4.0.2
alias of1912="source $HOME/OpenFOAM/OpenFOAM-v1912/etc/bashrc"
```

1.6. Save the changes to the .bashrc file and exit the text editor.

1.7. Restart the PARAM Sangnak supercomputer.

1.8. After the restart, use the **of1912** command to source the OpenFOAM environment in the terminal.

1.9. Change the current directory to **$HOME/OpenFOAM/ThirdParty-v1912** using the terminal (which

is already sourced with the **of1912** command).

1.10. Install the third-party packages by running the command:

```
./Allwmake
```

1.11. Change the current directory to **$HOME/OpenFOAM/OpenFOAM-v1912** using the terminal (which is already sourced with the **of1912** command).

1.12. Compile *OpenFOAM* by running the command: `./Allwmake -j`

Note: The compilation process may take several minutes to hours to complete.

2. Installing Foam-Extend 4.0 on PARAM Sangnak Supercomputer:

2.1. Create a folder called "foam" in your home directory.

2.2. Use the following commands to download the Foam-Extend 4.0 source files:

```
cd foam
git clone git://git.code.sf.net/p/foam-extend/foam-extend-4.0 foam-extend-4.0
```

2.3. Source the terminal environment by running the following commands:

```
cd ~/foam/foam-extend-4.0
source etc/bashrc
```

2.4. Enter your home directory and modify the .bashrc file similar to the installation of *OpenFOAM*-v1912. Replace the last line in the .bashrc file with:

```
alias fe40='source \$HOME/foam/foam-extend-4.0/etc/bashrc'
```

2.5. Save and exit the .bashrc file, and then restart your PARAM Sangnak account. 2.6. Source the terminal environment with the command **fe40**. 2.7. Change the directory to **~/foam/foam-extend-4.0** and start the compilation process by running the command:

```
./Allwmake.firstInstall
```

3. Installation of *solids4Foam* v1:

3.1. Create a folder named "FOAM_RUN."

3.2. Follow the commands below to install *solids4Foam*:

```
cd $FOAM_RUN
git clone https://bitbucket.org/philip_cardiff/solids4foam-release.git
cd solids4foam-release
./Allwmake
```

4. Sample script to run task on PARAM:

```
#!/bin/bash
#SBATCH -N 2
#SBATCH --job-name=beam_cross_flow
#SBATCH --ntasks-per-node=48
#SBATCH --partition=standard
#SBATCH --error=log.err
#SBATCH --output=log.out
#SBATCH --time=10:00:00

source solids4FoamScripts.sh
blockMesh -region solid
blockMesh -region fluid
decomposePar -region fluid
decomposePar -region solid
mpirun -np 12 solids4Foam -parallel
```

References

[1]. Tuković, E., Karač, A., Cardiff, P., Jasak, H., & Ivanković, A. (2018, October 19). OpenFOAM Finite Volume Solver for Fluid-Solid Interaction. *Transactions of FAMENA*, *42*(3), 1–31. https://doi.org/10.21278/tof.42301

[2]. Wu, Z., Ma, X., Brett, P. N., & Xu, J. (2009, January 20). Vibration analysis of submerged rectangular microplates with distributed mass loading. *Proceedings of the Royal Society A: Mathematical, Physical and Engineering Sciences*, *465*(2104), 1323–1336. https://doi.org/10.1098/rspa.2008.0447

[3]. Girfoglio, M., Quaini, A., & Rozza, G. (2021, January 1). Fluid-structure interaction simulations with a LES filtering approach in solids4Foam. *Communications in Applied and Industrial Mathematics*, *12*(1), 13–28. https://doi.org/10.2478/caim-2021-0002

[4]. Priambudi Setyo Pratomo, H., Dwiputra Suprianto, F., & Sutrisno, T. (2019). Preliminary Study on Mesh Stiffness Models for Fluid-structure Interaction Problems. *E3S Web of Conferences*, *130*, 01014. https://doi.org/10.1051/e3sconf/201913001014

[5]. Shayegh, A.: Block-coupled Finite Volume algorithms: A solids4Foam tutorial. In Proceedings of CFD with OpenSource Software, 2020, Edited by Nilsson. H., http://dx.doi.org/10.17196/OS_CFD#YEAR_2020

[6]. Tuković, E., Karač, A., Cardiff, P., Jasak, H., & Ivanković, A. (2018, October 19). OpenFOAM Finite Volume Solver for Fluid-Solid Interaction. *Transactions of FAMENA*, *42*(3), 1–31. https://doi.org/10.21278/tof.42301

[7]. Kanyanta, V., Ivankovic, A., & Karac, A. (2009, August). Validation of a fluid–structure interaction numerical model for predicting flow transients in arteries. *Journal of Biomechanics*, *42*(11), 1705–1712. https://doi.org/10.1016/j.jbiomech.2009.04.023

[8]. Cardiff, P., & Demirdžić, I. (2021, February 2). Thirty Years of the Finite Volume Method for Solid Mechanics. *Archives of Computational Methods in Engineering*, *28*(5), 3721–3780. https://doi.org/10.1007/s11831-020-09523-0

[9]. *Installation/Linux/foam-extend-4.0 - OpenFOAMWiki*. (n.d.). Installation/Linux/foam-extend-4.0 - OpenFOAMWiki. https://openfoamwiki.net/index.php/Installation/Linux/foam-extend-4.0

[10]. H. (2020, December 23). *How to install OpenFOAM v1912 from source pack*. CEMF.ir. https://www.cemf.ir/how-to-install-openfoam-v1912-from-source-pack/